Discrimination of Class I Cyclobutane Pyrimidine Dimer Photolyase from Blue Light Photoreceptors by Single Methionine Residue

Yuji Miyazawa,* Hirotaka Nishioka,† Kei Yura,‡§ and Takahisa Yamato*¶

*Graduate School of Science, Nagoya University, Nagoya 464-8602, Japan; †Graduate School of Environmental and Human Science, Meijo University, Nagoya 468-8502, Japan; ‡Quantum Bioinformatics Team, Center for Computational Science and Engineering, Japan Atomic Energy Agency, Kyoto 619-0215, Japan; §Research Unit for Quantum Beam Life Science Initiative, Quantum Beam Science Directorate, Japan Atomic Energy Agency, Kyoto 619-0215, Japan; and ¶CREST, Japan Science and Technology Agency, Saitama 332-0012, Japan

ABSTRACT DNA photolyase recognizes ultraviolet-damaged DNA and breaks improperly formed covalent bonds within the cyclobutane pyrimidine dimer by a light-activated electron transfer reaction between the flavin adenine dinucleotide, the electron donor, and cyclobutane pyrimidine dimer, the electron acceptor. Theoretical analysis of the electron-tunneling pathways of the DNA photolyase derived from *Anacystis nidulans* can reveal the active role of the protein environment in the electron transfer reaction. Here, we report the unexpectedly important role of the single methionine residue, Met-353, where busy trafficking of electron-tunneling currents is observed. The amino acid conservation pattern of Met-353 in the homologous sequences perfectly correlates with experimentally verified annotation as photolyases. The bioinformatics sequence analysis also suggests that the residue plays a pivotal role in biological function. Consistent findings from different disciplines of computational biology strongly suggest the pivotal role of Met-353 in the biological function of DNA photolyase.

INTRODUCTION

Ultraviolet (UV) light creates cyclobutane pyrimidine dimers (CPDs) in a DNA chain and causes skin cancer. DNA photolyase, containing a flavin cofactor, absorbs light and repairs the UV-damaged DNA using the electron transfer reaction between the electron donor (flavin adenine dinucleotide, $FADH^-$) and the electron acceptor (CPD) (1). Improperly formed covalent bonds in CPD are broken as a result of the electron transfer reaction, which is completed within 170 ps. To analyze the spatial pattern of electron-tunneling pathways, Medvedev and Stuchebrukhov proposed an electron-tunneling current and studied the electron transfer reaction of the computationally predicted complex structure of *Escherichia coli* DNA photolyase and CPD (2). They proposed a scheme of indirect electron transfer via the adenine of $FADH^-$ as a mediator of electron tunneling from the donor to the acceptor in their pioneering work on the CPD photolyase complex model. In 2004, Mees et al. reported the complex structure of the DNA photolyase derived from *Anacystis nidulans* and the CPD analog by x-ray crystallography (3). The isoalloxazine ring of the $FADH^-$ in the crystal structure is located close to the CPD, indicating the possibility of direct electron transfer from the $FADH^-$ to the CPD (4,5), and recent theoretical analyses support the direct transfer (6). An active role of the protein environment in electron transfer from the $FADH^-$* to the CPD has not been supported (1,7,8), but the possibility of protein-mediated electron transfer is not completely excluded.

Various methods for computation of the electronic factor in electron transfer reactions have been presented (9–11). Three major computational methods have been developed for the long-range electron transfer reactions in biological systems, namely, the extended Hückel approach used by Marcus and Stuchebrukhov (12) and expanded by Kakitani and coworkers (13–15), the pathway approach by Beratan and Onuchic (16), the square barrier model of Hopfield (17) promoted by Dutton (18), and the more intensive self-consistent field molecular orbital methods (19,20). In this study, we employed the extended Hückel approach to analyze the thermal fluctuation of electron-tunneling pathways for a large number of protein structures extracted from a molecular dynamics simulation trajectory.

It is widely accepted that the electronic factor for the electron transfer reaction fluctuates significantly along with the thermal fluctuation of the protein environment (15,21–24). Troisi et al. have made important contributions to the analysis of the effects of thermal fluctuations on the donor-acceptor couplings (25,26). Skourtis et al. have explicitly analyzed how thermal fluctuations affect the protein electron transfer (27). Recently, Nishioka et al. proposed a non-Condon theory for the electron transfer of thermally fluctuating protein media (28), and another study has analyzed the electron-tunneling pathways in a fixed protein environment (2). In this study, we used molecular dynamics simulation and quantum mechanical calculations to study the electron transfer reaction from the excited flavin cofactor to the thymine dimer in the explicit protein environment of a thermally fluctuating CPD photolyase complex (3). These calculations turned out to be helpful in identifying residues that are important in the electron transfer reaction. Furthermore, we

Submitted August 7, 2007, and accepted for publication November 5, 2007.

Address reprint requests to Takahisa Yamato, E-mail: yamato@phys.nagoya-u.ac.jp.

Editor: David P. Millar.

0006-3495/08/03/2194/10 $2.00

doi: 10.1529/biophysj.107.119248

used sequence database search techniques to evaluate the biological conservation of the key residues found by the analysis. As a result of the combined use of multiple disciplines of computational biology, we discovered that the methionine residue located at site 353 of *A. nidulans* CPD photolyase is a likely determinant for the function of class I CPD photolyase in the blue light photoreceptor superfamily.

MATERIALS AND METHODS

Molecular dynamics simulations and electronic structure calculations

The initial conformation of the complex of CPD analog and the DNA photolyase of *A. nidulans* was extracted from the Protein Data Bank (PDB code 1TEZ) (3). Crystallographic water molecules within the DNA photolyase and between the DNA photolyase and the CPD fragment were incorporated into the system. This system was then immersed in an octahedral box of water molecules. The total number of water molecules was 25,268. The AMBER99 force field (29) and the TIP3P model (30) were employed for the polypeptide chain and water molecules, respectively. The force field for the $FADH^-$, CPD analog, and 8-hydroxy-5-deazaflavin (8-HDF) were developed based on FADH(−), thymine dimer, and flavin mononucleotide (FMN) in the AMBER Parameter Database (http://pharmacy.man.ac.uk/amber), respectively. The atomic partial charges for these cofactors were calculated with the RESP scheme using the GAMESS (31) and AMBER8 (32) program packages. The 4-31G basis set was employed for this purpose. The bond lengths of the equilibrium conformation were adopted from the x-ray crystallographic values. The spring constants for the bond stretching and angles and dihedral torsional barriers were obtained from the AMBER parameter database. To construct the force field of the CPD analog, the structure of CPD was extracted from the PDB entry, 1SNH (33), and the $-O-P_2-O-$ part was replaced with $-O-CH_2-O-$. Structure optimization of the system was performed using the AMBER8 program with the harmonic restraints imposed on all nonhydrogen atoms in the system except for the solvent water molecules. These restraints were removed in the subsequent structure optimization processes. For the first stage of the molecular dynamics simulation, the temperature of the system was gradually elevated from 0 to 300 K during a time interval of 20 ps, with harmonic restraints imposed on all nonhydrogen atoms. Then, the *NPT* ensemble of the system was generated by the molecular dynamics simulation at $T = 300$ K, $P = 1$ atm without harmonic restraints for 1 ns. The time step for the simulation was 1 fs. The molecular dynamics simulation was performed by employing the octahedral boundary condition with the particle mesh Ewald method.

Electron-tunneling pathway analysis

The total electron-tunneling matrix element T_{if} consists of two parts, $T_{if} = T_{DA}^{dir} + T_{DA}$, where T_{DA}^{dir} is the direct term and T_{DA} is the tunneling matrix element via the mediator region between the donor and the acceptor. The direct term is given by $T_{DA}^{dir} = H_{DA} - ES_{DA}$, where H is the one-electron Hamiltonian, E is the tunneling energy, $H_{DA} = \langle \varphi_D | H | \varphi_A \rangle$, $S_{DA} = \langle \varphi_D | \varphi_A \rangle$, and ϕ_D, ϕ_A are the molecular orbitals of the donor and acceptor, respectively. We set the value of tunneling energy as the midpoint of the lowest unoccupied molecular orbital energy of the donor and the acceptor. The tunneling matrix element T_{DA} is given by the interatomic-tunneling currents as follows (34):

$$T_{DA} = \hbar \sum_{a \in \Omega_D^j, b \notin \Omega_D^j} J_{ab}, \quad (1)$$

where J_{ab} is the interatomic-tunneling current from atom a to atom b, and Ω_D^j is a donor separated from the acceptor side by plane j. The molecular orbitals Ψ_i(initial state) and Ψ_f(final state) determine the interatomic-tunneling current J_{ab} as

$$J_{ab} = \sum_{\mu \in a, \nu \in b} J_{\mu\nu},\ J_{\mu\nu} = \frac{1}{\hbar}(C_\mu^i C_\nu^f - C_\mu^f C_\nu^i)(H_{\mu\nu} - ES_{\mu\nu}), \quad (2)$$

where C_μ^i, C_ν^i are the coefficients of atomic orbitals ϕ_μ, ϕ_ν in Ψ_i, and C_μ^f, C_ν^f are the coefficients of atomic orbitals ϕ_μ, ϕ_ν in Ψ_f. The total electron population should be conserved throughout the reaction from the initial state to the final state. To impose this conservation condition, we scale the C_μ^i in Ψ_i (C_μ^f in Ψ_f) by multiplying $1/\sqrt{Pop^i}$ ($1/\sqrt{Pop^f}$), where $Pop^i = \sum_{n,m \in \text{all atomic orbital}} C_n^i S_{nm} C_m^i$, $Pop^f = \sum_{n,m \in \text{all atomic orbital}} C_n^f S_{nm} C_m^f$. To find the important region for long-range intramolecular electron tunneling, analysis of the interatomic-tunneling current J_{ab} is helpful. However, since the value of T_{DA} fluctuates as the thermal fluctuation of the protein, direct comparison of J_{ab} for different protein structures is not useful. To compare the significance of J_{ab} among different protein structures, we introduce the normalized tunneling current K_{ab} as $K_{ab} = \hbar J_{ab}/T_{DA}$. In the mediator region, the summation of the normalized tunneling current is always zero for a given atom, a, because the annihilation and creation of electrons do not take place. Therefore, the significance of electron tunneling cannot be evaluated for each atom with the normalized tunneling current. To evaluate the amount of the electron-tunneling current traffic, we introduce the electron-tunneling count (35) as $N_a = \hbar \sum_b' J_{ab}/|T_{DA}|$, where the summation $\sum'$ is taken over all positive tunneling currents J_{ab}. The electronic states of the donor, acceptor, protein, and the crystallographic waters are solved at the extended Hückel level. The extended Hückel parameters were taken from the literature (36), which are similar to those adopted by Stuchebrukhov et al. (37) in their previous work (2). We confirmed that the extended Hückel calculation with this parameterization reproduced a result similar to that of the previous work (2) for the fixed environment of the protein medium directly derived from x-ray crystallography (3). The value of T_{DA} is calculated by the pseudo-Green function technique (14,38) for each MD snapshot. The electron-tunneling pathways are analyzed by drawing the map of interatomic-tunneling currents (24).

To obtain the electron-tunneling pathways of CPD photolyase, we calculated electron-tunneling matrix elements and the interatomic electron-tunneling current for each of the instantaneous structures derived from the molecular dynamics simulation. When we calculate the tunneling matrix element T_{DA} for each protein conformation, we adopt a pruned protein, which consisted of $FADH^-$, CPD analog, Met-347-Ala-356, and Ala-384-Ser-393. In addition, 17 crystallographic waters were included in the system. The lowest unoccupied molecular orbital of the FMN part was considered the electron donor. The adenosine monophosphate part of the $FADH^-$ was included in the mediator region. The lowest unoccupied molecular orbital of the CPD analog was considered the electron acceptor. For this calculation,

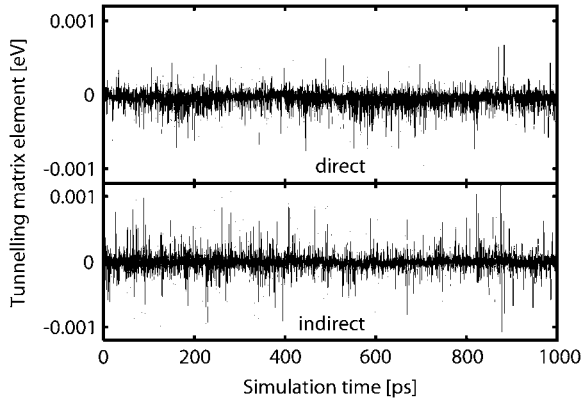

FIGURE 1 Fluctuation of electron-tunneling matrix element. The electron-tunneling matrix element is plotted as a function of simulation time at intervals of 100 fs for the direct term T_{DA}^{dir} (*top*) and the indirect term T_{DA} (*bottom*).

the CPD analog was truncated at the phosphate group. We confirmed that residues other than Met-347-Ala-356 and Ala-384-Ser-393 have little influence on the value of the indirect tunneling matrix element T_{DA}.

Multiple sequence alignment and dendrogram building

Amino acid sequences homologous to CPD photolyase from *A. nidulans* were searched for in UniProt (39) and in DDBJ (40) by BLAST (41) with default parameters. A multiple sequence alignment was built based on the progressive alignment method (42) using the BLOSUM62 matrix (43). Evolutionary distances between pairs of sequences were calculated based on the method by Kimura (44), and a dendrogram was made by the neighbor-joining method (45).

Selecting specifically conserved residues in a putative CPD photolyase subfamily

The sequences in the alignment were divided into two groups based on the type of amino acid residues at the site corresponding to site 353 of *A. nidulans* CPD photolyase (see Results and Discussion for the reason focusing on the site). The sequences with Met at site 353 were grouped as a putative CPD photolyase subfamily, and the sequences with non-Met at the site were grouped as a putative photoreceptor subfamily. The degree of conservation at every site in each group was calculated using information entropy based on the frequency of amino acid types at each site (46). A site in the putative CPD photolyase subfamily occupied by a single amino acid type with the entropy more than −1.72 was chosen as a well-conserved site. Information entropy of the corresponding sites in the putative photoreceptor subfamily was calculated, and all sites where the pattern of conservation in the two subfamilies was different were selected.

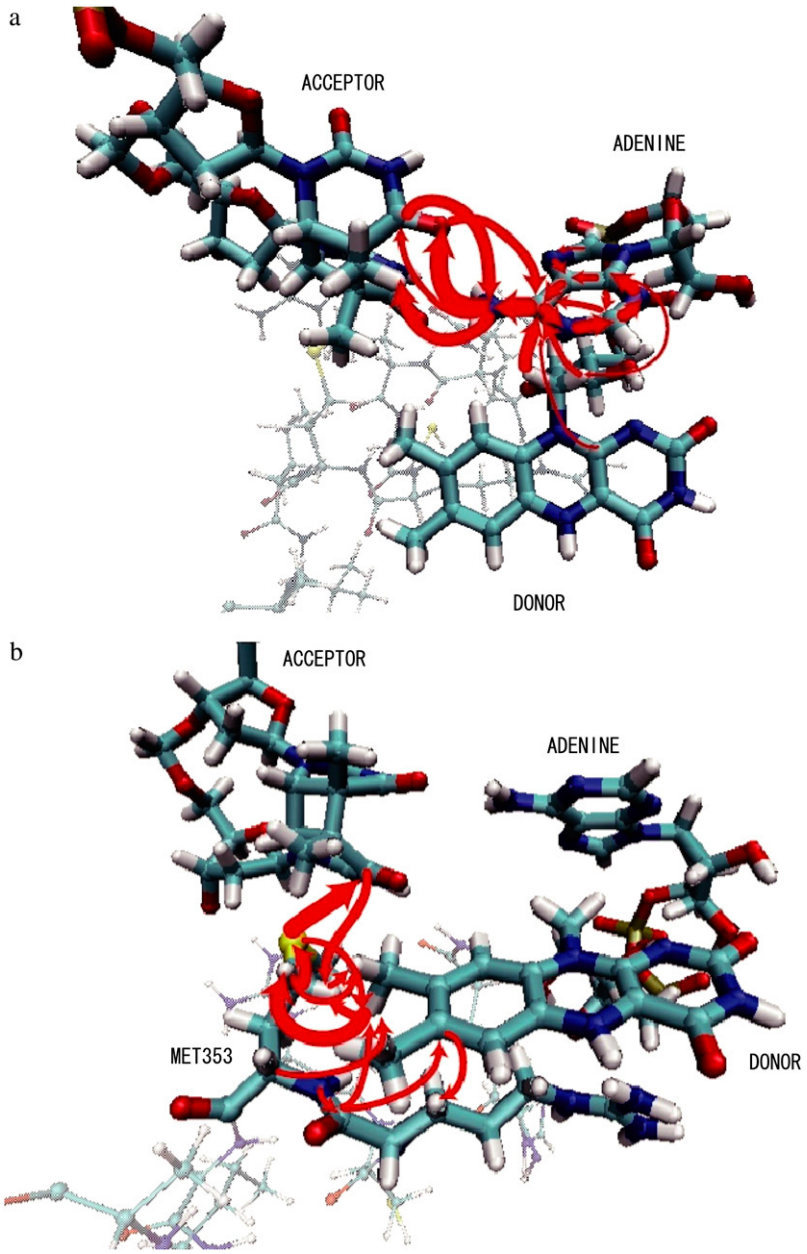

FIGURE 2 Electron-tunneling pathways. (*a*) Adenine route. (*b*) Met-353 route. Two typical electron-tunneling pathways are shown in these two panels. The width of each arrow is in proportion to the magnitude of the interatomic electron-tunneling current.

RESULTS AND DISCUSSION

Fluctuations of electron-tunneling matrix elements

In Fig. 1, the time series of electron-tunneling matrix elements shows significant fluctuation as the protein structure fluctuates on the energy landscape. It should be noted that the magnitude of T_{DA} is almost the same as that of the direct component of the tunneling matrix element, T_{DA}^{dir} ($\langle (T_{DA}^{dir})^2 \rangle = 1.32 \times 10^{-8} (eV)^2$, $\langle (T_{DA})^2 \rangle = 1.61 \times 10^{-8} (eV)^2$). Assuming the matching condition for the electron transfer reaction, the agreement between the theoretical value of the rate constant ($1.58 \times 10^9\ s^{-1}$) and the experimental value ($6.35 \times 10^9\ s^{-1}$) is strikingly good (4). An earlier experimental study reported that the electron-tunneling reaction from the excited flavin cofactor to the thymine dimer was completed in 170 ps (4). The theoretical analysis here indicates that the thermally fluctuating protein environment promotes an efficient electron transfer reaction in this protein-DNA complex.

To study the electron-tunneling mechanism of the DNA photolyase, Stuchebrukhov et al. (2) used a model system of the CPD-photolyase complex and the applied extended Hückel method for the electronic state calculations. They indicated that the adenine part plays an important role for the electron transfer reaction. In their calculations, they fixed atoms in the protein environment. Prytkova et al. (6) used the model system of the CPD-photolyase complex and applied advanced-level electronic state calculations. They implicitly considered the protein environment as an assembly of thermally fluctuating atomic point charges surrounding the donor-acceptor system. As a result, they indicate that the direct transfer plays a dominant role for the electron-tunneling reaction. In this study, however, we adopted the extended Hückel method, which provides a unique possibility for the explicit electronic state calculations of a large number of thermally fluctuating protein structures. Furthermore, we employed the realistic CPD-photolyase complex structure derived from x-ray crystallography (3). As a result, we found that the indirect electron transfer via the protein medium is as important as the direct electron transfer. Even though the calculation level is less accurate than the previous study (6), the present calculation adopted a more accurate description for the structure of the photolyase. The theoretical prediction derived from our theoretical calculations here will be strongly supported by the biological database analysis described in the later sections.

Electron-tunneling pathway

To analyze the electron-tunneling pathways in atomic detail, we calculated interatomic electron-tunneling currents for each of the instantaneous conformations of the protein-DNA complex derived from the molecular dynamics simulation. We found that there were two typical electron-tunneling routes for the electron transfer reaction of the CPD photolyase: an adenine route (Fig. 2 *a*) and a Met-353 route (Fig. 2 *b*). To evaluate the significance of each pathway in a quantitative manner, we analyzed the electron-tunneling count, which measures the amount of the electron-tunneling current traffic for each atom (47) (Fig. 3 *a*). Obviously, Asn-349, Met-353, Ala-385, and Gly-389 are candidate residues for electron-tunneling routes. It should be noted that care must be taken when interpreting the electron-tunneling count of each atom. For instance, destructive interference between interatomic electron-tunneling currents decreases the electronic factor of the rate constant (24). If a large number of tunneling currents are running in opposite directions to each other, the electronic factor of the rate constant should be small. In such a case, however, we often find atoms having large electron-tunneling count. To find typical pathways for the electron tunneling (Fig. 2), we inspected a large number of pathways that appeared in the molecular dynamics simulation trajectory. As a result, we found that the Met-353 pathways were more conspicuous than the other pathways involving Asn-349, Ala-385, and Gly-389.

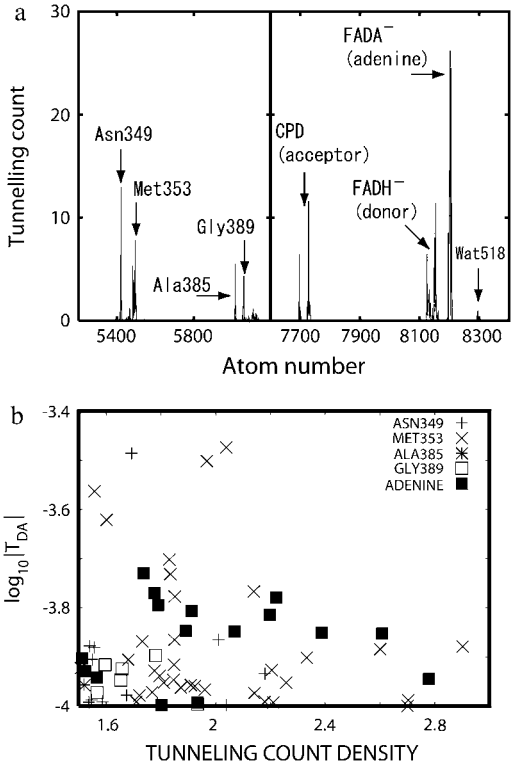

FIGURE 3 Electron-tunneling count. (*a*) The average electron-tunneling count is plotted as a function of the sequential number of atoms for the protein environment (*left*) and the donor-acceptor region (*right*). Important regions are indicated by arrows. (*b*) For Asn-349, Met-353, Ala-385, Gly-389, and the adenine part of $FADH^-$, the tunneling count density, defined by the total tunneling count of the constituent atoms divided by the number of heavy atoms, is calculated. The values of tunneling count density were evaluated for 10,000 different protein structures derived from the molecular dynamics simulation trajectory. We focus on the high-density regime where the tunneling count density is ≥ 1.5. In this regime, $\log_{10}|T_{DA}|$ was plotted against the tunneling count density for the large $|T_{DA}|$, ($\log_{10}|T_{DA}| \geq 4.0$).

To evaluate the role of the protein environment in the electron-tunneling reaction more quantitatively, we analyzed the correlation between the tunneling count of the different parts of the mediator and T_{DA} (Fig. 3 *b*). Clearly, the contribution of Met-353 to T_{DA} is comparable to that of the adenine part, and the significance of Met-353 is much greater than that of Asn-349, Ala-385, and Gly-389. Fig. 3 *b* shows that the electron-tunneling matrix element, T_{DA}, tends to be large when the tunneling count density of Met-353 is large (high-coupling, high-density regime). It is supposed that, in general, the electron transfer reaction takes place when the magnitude of the electronic factor is large during the thermal fluctuation of the system. Therefore, the high-coupling, high-density regime is important for the reaction. On the other hand, in the low-coupling, high-density regime, the destructive interference between electron-tunneling currents decreases the magnitude of the electronic factor. We analyzed the correlation between T_{DA} and the tunneling current density in the low-coupling, high-density regime and recognized no significant difference of the correlation among Asn-349, Met-353, Ala-385, Gly-389, and the adenine part, indicating that the destructive interference between electron-tunneling currents is probable in any part of the mediator regions.

Importance of Met-353 for photorepair function

Among the sequences similar to that of *A. nidulans* CPD photolyase, 201 out of 371 have Met at the site corresponding to 353 of *A. nidulans* CPD photolyase. In a dendrogram drawn based on Kimura's distance (44) by the neighbor-joining

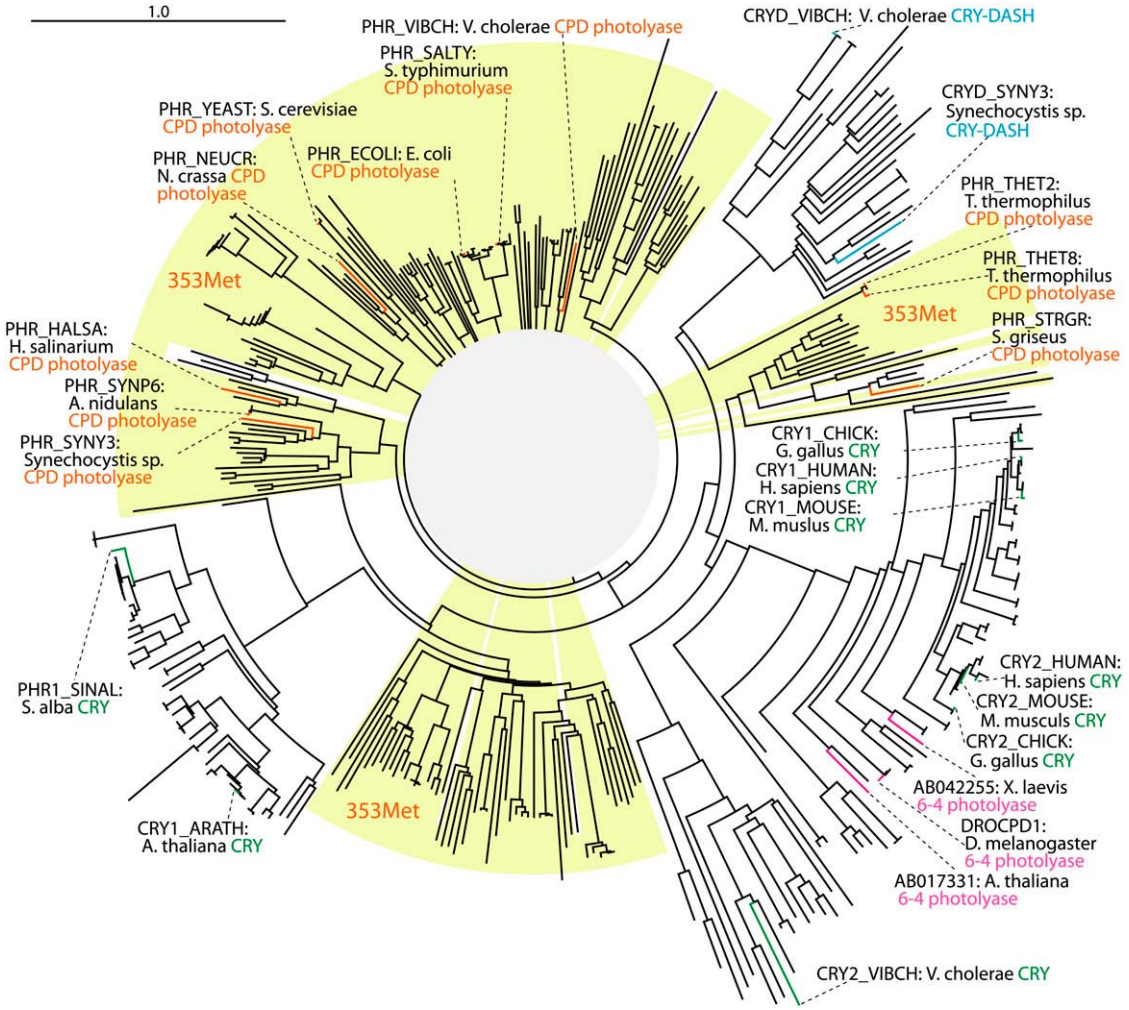

FIGURE 4 A dendrogram based on amino acid sequences in the photolyase blue light photoreceptor family. A root of the dendrogram was located in the gray circle at the center, but the exact location is unclear because of uncertainty in the branching order of the dendrogram. A branch with a yellow background represents amino acid sequences with Met at the site corresponding to 353 of *A. nidulans* CPD photolyase. For protein sequences with experimentally verified biological function, the protein (gene) ID and species and protein names are shown. A protein with its name in orange has CPD repair function, a protein in green has biological functions related to CRY, a protein in cyan has functions related to CRY-DASH, and a protein in pink has 6-4 photoproduct repair function. The bar at the top left represents a branch length that corresponds to 1.0 amino acid substitutions per site based on Kimura's distance.

method (45), proteins with Met at site 353 were clustered into three groups (Fig. 4). The small groups may have arisen because of ambiguity in amino acid sequence alignment, and a majority of the sequences was clustered into one large group.

CPD photolyase belongs to the photolyase blue light photoreceptor family (48), which consists of classes I and II CPD photolyases, cryptochrome (CRY), and cryptochrome from *Drosophila*, *Arabidopsis*, *Synechocystis*, and *Homo* (CRY-DASH) (49). CPD photolyases of classes I and II repair CPD on UV-damaged DNA; the former has been isolated from eubacteria and fungi, whereas the latter is widely distributed throughout all organisms (50,51). In this study, class II CPD photolyase is omitted due to its low sequence identity to class I photolyase. CRY proteins in plants are responsible for the regulation of seedling growth and the flowering season (52), whereas CRY proteins in animals are known to be involved in the circadian rhythm (53). These CRY proteins do not show detectable photorepair activity of UV-damaged DNA. The 6-4 photolyase proteins, showing high sequence similarity to the CRY subfamily, repair 6-4 photoproducts selectively (49). A protein in the CRY-DASH subfamily was reported to bind DNA nonspecifically and was suggested to function as a transcriptional regulator in a cyanobacterium (54). A protein was initially shown to possess no detectable photorepair activity of UV-damaged DNA (55) but recently has been shown to repair CPD in single-stranded DNA, not in double-stranded DNA (56).

Those biological functions of proteins in the family were found to have perfect correlation with the existence of Met at site 353 (Table 1). Proteins in the photolyase blue light photoreceptor family experimentally verified to have CPD repair activity on double-stranded DNA always have Met at site 353, and proteins related to photoreceptor or circadian rhythm activities have an amino acid residue other than Met at the site. Amino acid sequence comparison also suggests

TABLE 1 Experimentally verified function of protein coded by photolyase blue light photoreceptor family gene and amino acid residue at residue number 353

Sequence ID	Species	Verified function	aa at 353
Class I CPD photolyase subfamily:			
PHR_ECOLI (60)	*Escherichia coli*	Catalyze the light-dependent monomerization of CPD	Met
PHR_SALTY (61)	*Salmonella typhimurium*	Catalyze the light-dependent monomerization of CPD	Met
PHR_THET2 (62)	*Thermus thermophilus*	Catalyze the light-dependent monomerization of CPD	Met
PHR_THET8 (63)	*T. thermophilus*	Bind CPD	Met
PHR_VIBCH (64)	*Vibrio cholerae*	Bind CPD, involved in repair	Met
PHR_STRGR (65)	*Streptomyces griseus*	Complement phr-deficient *E. coli*	Met
PHR_HALSA (66)	*Halobacterium salinarium*	Complement phr-deficient *E. coli*	Met
PHR_SYNP6 (67)	*Anacystis nidulans*	Complement phr-deficient *E. coli*	Met
PHR_SYNY3 (55)	*Synechocystis* sp.	Complement phr-deficient *E. coli*, involved in repair of UV radiation-induced DNA damage	Met
PHR_YEAST (68)	*Saccharomyces cerevisiae*	Catalyze the light-dependent monomerization of CPD	Met
PHR_NEUCR (69)	*Neurospora crassa*	Complement phr-deficient *E. coli*	Met
CRY subfamily:			
CRY1_HUMAN (70)	*Homo sapiens*	Circadian clock component, negatively regulate *Per1* transcription independent of light	His
CRY2_HUMAN (70)	*H. sapiens*	Circadian clock component, negatively regulate *Per1* transcription independent of light	His
CRY1_MOUSE (71)	*Mus musculus*	Blue light-dependent regulator of the circadian feedback loop, no photolyase activity	His
CRY2_MOUSE (71)	*M. musculus*	Blue light-dependent regulator of the circadian feedback loop, no photolyase activity	His
CRY1_CHICK (72)	*Gallus gallus*	Blue light-dependent regulator of the circadian feedback loop, no photolyase activity	His
CRY2_CHICK (72)	*G. gallus*	Blue light-dependent regulator of the circadian feedback loop, no photolyase activity	His
CRY1_ARATH (73)	*Arabidopsis thaliana*	Mediate blue light-induced gene expression	Val
CRY2_VIBCH (64)	*V. cholerae*	No photolyase activity	Ala
PHR1_SINAL (57,58)	*S. alba*	No photolyase activity	Val
6-4 photolyase subfamiliy:			
DROCPD1 (74)	*Drosophila melanogaster*	Complement phr-deficient *E. coli*, 6-4 photolyase	His
AB042255(75)	*Xenopus laevis*	Complement phr-deficient *E. coli*, 6-4 photolyase	His
AB017331(76)	*A. thaliana*	Complement phr-deficient *E. coli*, 6-4 photolyase	His
CRY-DASH subfamiliy:			
CRYD_SYNY3 (54)	*Synechocystis* sp.	Bind DNA, repress transcription of eight genes	Gln
CRYD_VIBC (56,64)	*V. cholerae*	Bind RNA, photolyase activity on single-stranded DNA	Gln

that Met at site 353 plays an important role for repairing CPD on double-stranded DNA.

A member of the photolyase blue light photoreceptor family from *Sinapis alba* (PHR1_SINAL) has Val at site 353 but is annotated as CPD photolyase in UniProt (39). This annotation is based on an experiment that photolyase-deficient *E. coli* restored photorepair activity by introducing the gene from *S. alaba* (57). Malhotra et al. (58) later challenged the notion that PHR1_SINAL undergoes DNA repair activity and proved that the protein lacked this function. Our analyses support the latter experimental results. The sequence does not have Met at site 353, and the dendrogram analysis showed that the sequence was grouped in the CRY subfamily (Fig. 4).

In the multiple sequence alignment, 12 amino acid residue sites have an amino acid conservation pattern similar to that of Met-353 (Fig. 5 *a, opaque residues*). In the putative CPD photolyase subfamily, in which proteins have Met at site 353, these 12 sites were occupied by well-conserved residues; however, in the putative photoreceptor subfamily, the corresponding 12 sites were not conserved or were conserved as an amino acid type different from that in the putative CPD photolyase subfamily. This subfamily-specific conservation of amino acid residues suggests that these are the functionally important sites. These sites were, in three-dimensional space, located at the interface between $FADH^-$ and DNA and surrounded Met-353 (Fig. 5 *b*), where electron transfer from $FADH^-$ to CPD occurs. The pivotal residue for electron transfer function indicated by the protein dynamics simulation helped in identifying the specific amino acid conservation pattern in the putative CPD photolyase subfamily, which is responsible for maintaining the electron transfer pathway (Fig. 5 *b*). The fact that the residues uniquely conserved in the putative CPD photolyase subfamily mostly include the pruned protein residues we used for electron transfer calculation reinforces the possible role of these conserved residues.

6-4 photolyase, which repairs the 6-4 product, was shown to be derived from the CRY subfamily (49). CRY proteins have been shown to possess no photolyase activity (Table 1), and 6-4 photolyase has therefore acquired 6-4 repair activity at some point during its molecular evolution. 6-4 photolyase has His, not Met, at site 353, and it has been proposed that the His residue plays an active role in the (6-4)-specific reaction (1). We would also suggest here that the electron transfer pathway of 6-4 repair is likely to be different from that of CPD repair.

Selby and Sancar (56) demonstrated that CRY-DASH is a photolyase with specificity on CPD in single-stranded DNA but not in double-stranded DNA. In the multiple sequence alignment, Met at site 353 of *A. nidulans* class I CPD pho-

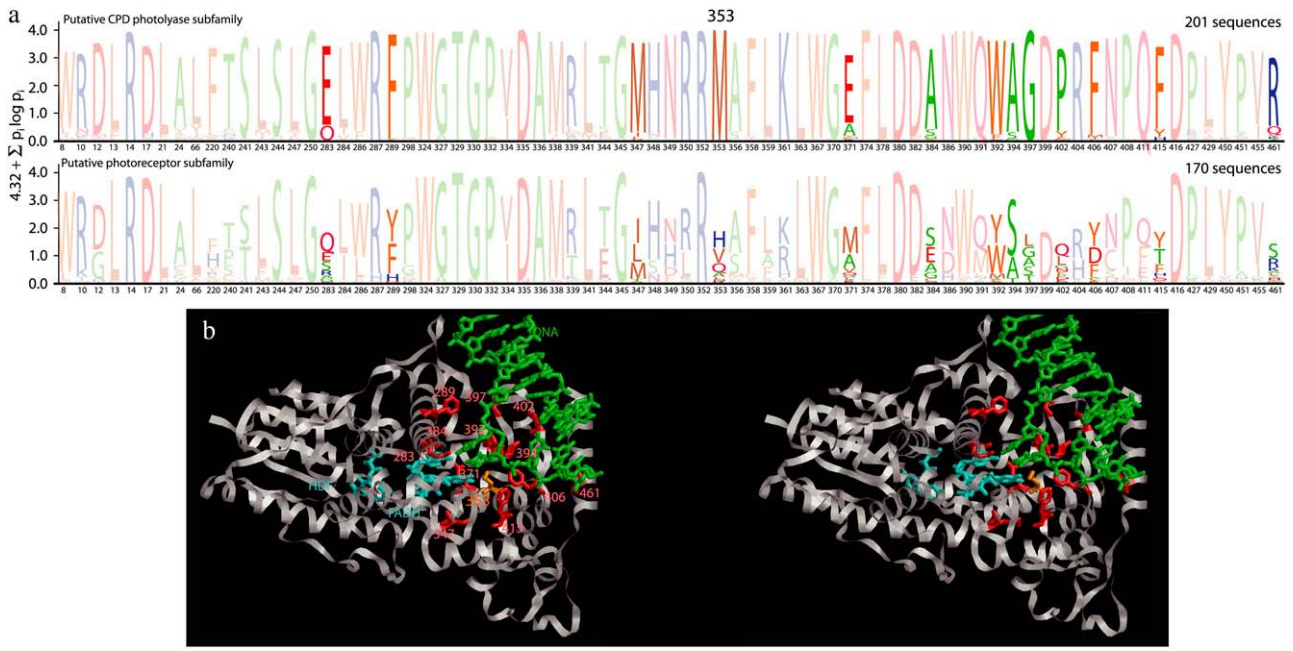

FIGURE 5 Evolutionarily conserved residues in protein structures. (*a*) Sites in the amino acid sequence that have similar conservation pattern to Met-353 of *A. nidulans* CPD photolyase. The putative CPD photolyase subfamily includes sequences with Met at site 353 (201 sequences), and the remaining sequences are grouped as a putative photoreceptor subfamily (170 sequences). All sites with information entropy more than −1.72 (>2.6 on the *vertical axis*) are shown. Among them, sites with the same amino acid conservation pattern between the two subfamilies are shown in translucent color, and sites with different conservation patterns are opaque. The numbers on the horizontal axis are residue numbers in *A. nidulans* CPD photolyase. (*b*) Sites with an amino acid conservation pattern specific to the putative CPD photolyase subfamily (*opaque sites* in *a*) are shown in red bold in the stereo drawing of the *A. nidulans* CPD photolyase with damaged DNA (*green*). 8-HDF and $FADH^-$ are shown in cyan. Met-353 is shown in orange. All the residues specifically conserved in the putative CPD photolyase subfamily are located between the electron donor FADH and electron acceptor DNA.

tolyase is replaced to Gln in CRY-DASH. We, therefore, suggest that the electron transfer pathway for repairing CPD on single-stranded DNA by CRY-DASH is not the same as the one for repairing CPD on double-stranded DNA by class I CPD photolyase. X-ray crystallographic study of CRY-DASH showed that the characteristics of the DNA interface of CRY-DASH are different from those of class I CPD photolyase, reflecting the differences of substrate (59). The differences in structure of the substrate DNA may result in differences in positions to bind CPD on the photolyase surface and end in differentiating the residue's role at site 353.

CONCLUSIONS

We studied the role of the protein environment and its fluctuations in the biological function of the CPD photolyase derived from *A. nidulans*. For this purpose, we used molecular dynamics simulation and quantum mechanical calculations to analyze the electron transfer reaction from the excited flavin cofactor to the thymine dimer in the explicit protein environment of the thermally fluctuating CPD photolyase complex. The results showed that indirect electron tunneling via the protein medium is as important as direct electron transfer from the donor to the acceptor. We also observed busy electron-tunneling traffic at the Met-353 site. Furthermore, we used bioinformatics techniques to evaluate the evolutionary conservation of the key residues found by the analysis. We found that Met-353 of the CPD photolyase derived from *A. nidulans* has been perfectly conserved throughout the putative class I CPD photolyases.

The computations were performed at computer centers at Nagoya University, the Institute for Molecular Science, and the Japan Atomic Energy Agency.

This work was supported by a Grant-in-Aid for the 21st Century COE program Frontiers of Computational Science, and Research Foundation for Opto-Science and Technology to T.Y. K.Y. was partly supported by a Grant-in-Aid for Scientific Research (C) from the Japan Society for the Promotion of Science (JSPS) KAKENHI (16570138).

REFERENCES

1. Sancar, A. 2003. Structure and function of DNA photolyase and cryptochrome blue-light photoreceptors. *Chem. Rev.* 103:2203–2237.
2. Medvedev, D., and A. A. Stuchebrukhov. 2001. DNA repair mechanism by photolyase: electron transfer path from the photolyase catalytic cofactor FADH(−) to DNA thymine dimer. *J. Theor. Biol.* 210: 237–248.
3. Mees, A., T. Klar, P. Gnau, U. Hennecke, A. P. Eker, T. Carell, and L. O. Essen. 2004. Crystal structure of a photolyase bound to a CPD-like DNA lesion after in situ repair. *Science.* 306:1789–1793.
4. Kao, Y. T., C. Saxena, L. Wang, A. Sancar, and D. Zhong. 2005. Direct observation of thymine dimer repair in DNA by photolyase. *Proc. Natl. Acad. Sci. USA.* 102:16128–16132.
5. Li, J., T. Uchida, T. Todo, and T. Kitagawa. 2006. Similarities and differences between cyclobutane pyrimidine dimer photolyase and (6–4) photolyase as revealed by resonance Raman spectroscopy: electron transfer from the FAD cofactor to ultraviolet-damaged DNA. *J. Biol. Chem.* 281:25551–25559.
6. Prytkova, T. R., D. N. Beratan, and S. S. Skourtis. 2007. Photoselected electron transfer pathways in DNA photolyase. *Proc. Natl. Acad. Sci. USA.* 104:802–807.
7. Byrdin, M., V. Sartor, A. P. Eker, M. H. Vos, C. Aubert, K. Brettel, and P. Mathis. 2004. Intraprotein electron transfer and proton dynamics during photoactivation of DNA photolyase from E. coli: review and new insights from an ''inverse'' deuterium isotope effect. *Biochim. Biophys. Acta.* 1655:64–70.
8. Weber, S. 2005. Light-driven enzymatic catalysis of DNA repair: a review of recent biophysical studies on photolyase. *Biochim. Biophys. Acta.* 1707:1–23.
9. Newton, M. D. 1991. Quantum chemical probes of electron-transfer kinetics—the nature of donor-acceptor interactions. *Chem. Rev.* 91:767–792.
10. Newton, M. D., and R. J. Cave. 1997. Molecular control of electron and hole transfer processes: electronic structure theory and application. *In* Molecular Electronics, Chemistry for the 21st Century. J. Jortner and M. A. Ratner, editors. Blackwell, Malden, MA. 73–118.
11. Skourtis, S. S., and D. N. Beratan. 1999. Theories of structure-function relationships for bridge-mediated electron transfer reactions. *Adv. Chem. Phys.* 106:377–452.
12. Stuchebrukhov, A. A., and R. A. Marcus. 1995. Theoretical study of electron transfer in ferrocytochromes. *J. Phys. Chem.* 99:7581–7590.
13. Kawatsu, T., T. Kakitani, and T. Yamato. 2000. A novel method for determining the electron tunneling pathway in protein. *Inorg. Chim. Acta.* 300:862–868.
14. Kawatsu, T., T. Kakitani, and T. Yamato. 2002. On the anomaly of the tunneling matrix element in long-range electron transfer. *J. Phys. Chem. B.* 106:5068–5074.
15. Nishioka, H., A. Kimura, T. Yamato, T. Kawatsu, and T. Kakitani. 2005. Interference, fluctuation, and alternation of electron tunneling in protein media. 1. Two tunneling routes in photosynthetic reaction center alternate due to thermal fluctuation of protein conformation. *J. Phys. Chem. B.* 109:1978–1987.
16. Beratan, D. N., J. N. Betts, and J. N. Onuchic. 1991. Protein electron transfer rates set by the bridging secondary and tertiary structure. *Science.* 252:1285–1288.
17. Hopfield, J. J. 1974. Electron transfer between biological molecules by thermally activated tunneling. *Proc. Natl. Acad. Sci. USA.* 71:3640–3644.
18. Page, C. C., C. C. Moser, X. X. Chen, and P. L. Dutton. 1999. Natural engineering principles of electron tunnelling in biological oxidation-reduction. *Nature.* 402:47–52.
19. Kurnikov, I. V., and D. N. Beratan. 1996. Ab initio based effective Hamiltonians for long-range electron transfer: Hartree-Fock analysis. *J. Chem. Phys.* 105:9561–9573.
20. Stuchebrukhov, A. A. 2001. Toward ab initio theory of long-distance electron tunneling in proteins: tunneling currents approach. *Adv. Chem. Phys.* 118:1–44.
21. Prytkova, T. R., I. V. Kurnikov, and D. N. Beratan. 2007. Coupling coherence distinguishes structure sensitivity in protein electron transfer. *Science.* 315:622–625.
22. Daizadeh, I., E. S. Medvedev, and A. A. Stuchebrukhov. 1997. Effect of protein dynamics on biological electron transfer. *Proc. Natl. Acad. Sci. USA.* 94:3703–3708.
23. Balabin, I. A., and J. N. Onuchic. 2000. Dynamically controlled protein tunneling paths in photosynthetic reaction centers. *Science.* 290: 114–117.
24. Kawatsu, T., T. Kakitani, and T. Yamato. 2002. Destructive interference in the electron tunneling through protein media. *J. Phys. Chem. B.* 106:11356–11366.
25. Troisi, A., A. Nitzan, and M. A. Ratner. 2003. A rate constant expression for charge transfer through fluctuating bridges. *J. Chem. Phys.* 119:5782–5788.
26. Troisi, A., M. A. Ratner, and M. B. Zimmt. 2004. Dynamic nature of the intramolecular electronic coupling mediated by a solvent molecule: a computational study. *J. Am. Chem. Soc.* 126:2215–2224.

27. Skourtis, S. S., I. A. Balabin, T. Kawatsu, and D. N. Beratan. 2005. Protein dynamics and electron transfer: electronic decoherence and non-Condon effects. *Proc. Natl. Acad. Sci. USA.* 102:3552–3557.

28. Nishioka, H., A. Kimura, T. Yamato, T. Kawatsu, and T. Kakitani. 2005. Interference, fluctuation, and alternation of electron tunneling in protein media. 2. Non-Condon theory for the energy gap dependence of electron transfer rate. *J. Phys. Chem. B.* 109:15621–15635.

29. Ponder, J. W., and D. A. Case. 2003. Force fields for protein simulations. *Adv. Protein Chem.* 66:27–85.

30. Jorgensen, W. L., J. Chandrasekhar, J. D. Madura, R. W. Impey, and M. L. Klein. 1983. Comparison of simple potential functions for simulating liquid water. *J. Chem. Phys.* 79:926–935.

31. Schmidt, M. W., K. K. Baldridge, J. A. Boatz, S. T. Elbert, M. S. Gordon, J. H. Jensen, S. Koseki, N. Matsunaga, K. A. Nguyen, S. J. Su, T. L. Windus, M. Dupuis, and J. A. Montgomery. 1993. General atomic and molecular electronic-structure system. *J. Comput. Chem.* 14:1347–1363.

32. Case, D. A., T. A. Darden, T. E. Cheatham III, C. L. Simmerling, J. Wang, R. E. Duke, R. Luo, K. M. Merz, D. A. Pearlman, M. Crowley, R. C. Walker, W. Zhang, B. Wang, S. Hayik, A. Roitberg, G. Seabra, K. F. Wong, F. Paesani, X. Wu, S. Brozell, V. Tsui, H. Gohlke, L. Yang, C. Tan, J. Mongan, V. Hornak, G. Cui, P. Beroza, D. H. Mathews, C. Schafmeister, W. S. Ross, and P. A. Kollman. 2004. AMBER 8. University of California, San Francisco.

33. Lee, J. H., C. J. Park, J. S. Shin, T. Ikegami, H. Akutsu, and B. S. Choi. 2004. NMR structure of the DNA decamer duplex containing double T·G mismatches of *cis-syn* cyclobutane pyrimidine dimer: implications for DNA damage recognition by the XPC-hHR23B complex. *Nucleic Acids Res.* 32:2474–2481.

34. Stuchebrukhov, A. A. 1996. Tunneling currents in electron transfer reaction in proteins. 2. Calculation of electronic superexchange matrix element and tunneling currents using nonorthogonal basis sets. *J. Chem. Phys.* 105:10819–10829.

35. Cheung, M. S., I. Daizadeh, A. A. Stuchebrukhov, and P. F. Heelis. 1999. Pathways of electron transfer in Escherichia coli DNA photolyase: Trp(306) to FADH. *Biophys. J.* 76:1241–1249.

36. Anderson, A. B., and E. Grantscharova. 1995. Catalytic effect of ruthenium in ruthenium-platinum alloys on the electrodooxidation of methanol: molecular-orbital theory. *J. Phys. Chem.* 99:9149–9154.

37. Alvarez, S. 1995. Tables of Parameters for Extended Huckel Calculations. Universitat de Barcelona, Barcelona, Spain.

38. Stuchebrukhov, A. A. 1994. Dispersion-relations for electron and hole transfer in donor bridge acceptor systems. *Chem. Phys. Lett.* 225:55–61.

39. The UniProt Consortium. 2007. The Universal Protein Resource (UniProt). *Nucleic Acids Res.* 35:D193–D197.

40. Sugawara, H., T. Abe, T. Gojobori, and Y. Tateno. 2007. DDBJ working on evaluation and classification of bacterial genes in INSDC. *Nucleic Acids Res.* 35:D13–D15.

41. Altschul, S. F., T. L. Madden, A. A. Schaffer, J. Zhang, Z. Zhang, W. Miller, and D. J. Lipman. 1997. Gapped BLAST and PSI-BLAST: a new generation of protein database search programs. *Nucleic Acids Res.* 25:3389–3402.

42. Barton, G. J., and M. J. Sternberg. 1987. A strategy for the rapid multiple alignment of protein sequences. Confidence levels from tertiary structure comparisons. *J. Mol. Biol.* 198:327–337.

43. Henikoff, S., and J. G. Henikoff. 1992. Amino acid substitution matrices from protein blocks. *Proc. Natl. Acad. Sci. USA.* 89:10915–10919.

44. Kimura, M. 1983. The Neutral Theory of Molecular Evolution. Cambridge University Press, Cambridge, UK.

45. Saitou, N., and M. Nei. 1987. The neighbor-joining method: a new method for reconstructing phylogenetic trees. *Mol. Biol. Evol.* 4: 406–425.

46. Schneider, T. D., and R. M. Stephens. 1990. Sequence logos: a new way to display consensus sequences. *Nucleic Acids Res.* 18:6097–6100.

47. Stuchebrukhov, A. A. 1996. Tunneling currents in electron transfer reactions in proteins. *J. Chem. Phys.* 104:8424–8432.

48. Kanai, S., R. Kikuno, H. Toh, H. Ryo, and T. Todo. 1997. Molecular evolution of the photolyase-blue-light photoreceptor family. *J. Mol. Evol.* 45:535–548.

49. Daiyasu, H., T. Ishikawa, K. Kuma, S. Iwai, T. Todo, and H. Toh. 2004. Identification of cryptochrome DASH from vertebrates. *Genes Cells.* 9:479–495.

50. Sancar, G. B. 1990. DNA photolyases: physical properties, action mechanism, and roles in dark repair. *Mutat. Res.* 236:147–160.

51. Yasui, A., A. P. Eker, S. Yasuhira, H. Yajima, T. Kobayashi, M. Takao, and A. Oikawa. 1994. A new class of DNA photolyases present in various organisms including aplacental mammals. *EMBO J.* 13: 6143–6151.

52. Ahmad, M., and A. R. Cashmore. 1993. HY4 gene of A. thaliana encodes a protein with characteristics of a blue-light photoreceptor. *Nature.* 366:162–166.

53. Rosato, E., V. Codd, G. Mazzotta, A. Piccin, M. Zordan, R. Costa, and C. P. Kyriacou. 2001. Light-dependent interaction between Drosophila CRY and the clock protein PER mediated by the carboxy terminus of CRY. *Curr. Biol.* 11:909–917.

54. Brudler, R., K. Hitomi, H. Daiyasu, H. Toh, K. Kucho, M. Ishiura, M. Kanehisa, V. A. Roberts, T. Todo, J. A. Tainer, and E. D. Getzoff. 2003. Identification of a new cryptochrome class. Structure, function, and evolution. *Mol. Cell.* 11:59–67.

55. Hitomi, K., K. Okamoto, H. Daiyasu, H. Miyashita, S. Iwai, H. Toh, M. Ishiura, and T. Todo. 2000. Bacterial cryptochrome and photolyase: characterization of two photolyase-like genes of Synechocystis sp. PCC6803. *Nucleic Acids Res.* 28:2353–2362.

56. Selby, C. P., and A. Sancar. 2006. A cryptochrome/photolyase class of enzymes with single-stranded DNA-specific photolyase activity. *Proc. Natl. Acad. Sci. USA.* 103:17696–17700.

57. Batschauer, A. 1993. A plant gene for photolyase: an enzyme catalyzing the repair of UV-light-induced DNA damage. *Plant J.* 4: 705–709.

58. Malhotra, K., S. T. Kim, A. Batschauer, L. Dawut, and A. Sancar. 1995. Putative blue-light photoreceptors from Arabidopsis thaliana and Sinapis alba with a high degree of sequence homology to DNA photolyase contain the two photolyase cofactors but lack DNA repair activity. *Biochemistry.* 34:6892–6899.

59. Huang, Y., R. Baxter, B. S. Smith, C. L. Partch, C. L. Colbert, and J. Deisenhofer. 2006. Crystal structure of cryptochrome 3 from Arabidopsis thaliana and its implications for photolyase activity. *Proc. Natl. Acad. Sci. USA.* 103:17701–17706.

60. Johnson, J. L., S. Hamm-Alvarez, G. Payne, G. B. Sancar, K. V. Rajagopalan, and A. Sancar. 1988. Identification of the second chromophore of Escherichia coli and yeast DNA photolyases as 5,10-methenyltetrahydrofolate. *Proc. Natl. Acad. Sci. USA.* 85:2046–2050.

61. Li, Y. F., and A. Sancar. 1991. Cloning, sequencing, expression and characterization of DNA photolyase from Salmonella typhimurium. *Nucleic Acids Res.* 19:4885–4890.

62. Kato, R., K. Hasegawa, Y. Hidaka, S. Kuramitsu, and T. Hoshino. 1997. Characterization of a thermostable DNA photolyase from an extremely thermophilic bacterium, Thermus thermophilus HB27. *J. Bacteriol.* 179:6499–6503.

63. Torizawa, T., T. Ueda, S. Kuramitsu, K. Hitomi, T. Todo, S. Iwai, K. Morikawa, and I. Shimada. 2004. Investigation of the cyclobutane pyrimidine dimer (CPD) photolyase DNA recognition mechanism by NMR analyses. *J. Biol. Chem.* 279:32950–32956.

64. Worthington, E. N., I. H. Kavakli, G. Berrocal-Tito, B. E. Bondo, and A. Sancar. 2003. Purification and characterization of three members of the photolyase/cryptochrome family glue-light photoreceptors from Vibrio cholerae. *J. Biol. Chem.* 278:39143–39154.

65. Kobayashi, T., M. Takao, A. Oikawa, and A. Yasui. 1989. Molecular characterization of a gene encoding a photolyase from Streptomyces griseus. *Nucleic Acids Res.* 17:4731–4744.

66. Takao, M., T. Kobayashi, A. Oikawa, and A. Yasui. 1989. Tandem arrangement of photolyase and superoxide dismutase genes in Halobacterium halobium. *J. Bacteriol.* 171:6323–6329.

67. Yasui, A., M. Takao, A. Oikawa, A. Kiener, C. T. Walsh, and A. P. Eker. 1988. Cloning and characterization of a photolyase gene from the cyanobacterium Anacystis nidulans. *Nucleic Acids Res.* 16:4447–4463.

68. Baer, M. E., and G. B. Sancar. 1993. The role of conserved amino acids in substrate binding and discrimination by photolyase. *J. Biol. Chem.* 268:16717–16724.

69. Yajima, H., H. Inoue, A. Oikawa, and A. Yasui. 1991. Cloning and functional characterization of a eucaryotic DNA photolyase gene from Neurospora crassa. *Nucleic Acids Res.* 19:5359–5362.

70. Griffin, E. A. Jr., D. Staknis, and C. J. Weitz. 1999. Light-independent role of CRY1 and CRY2 in the mammalian circadian clock. *Science.* 286:768–771.

71. Kondratov, R. V., A. A. Kondratova, C. Lee, V. Y. Gorbacheva, M. V. Chernov, and M. P. Antoch. 2006. Post-translational regulation of circadian transcriptional CLOCK(NPAS2)/BMAL1 complex by cryptochromes. *Cell Cycle.* 5:890–895.

72. Yamamoto, K., T. Okano, and Y. Fukada. 2001. Chicken pineal CRY genes: light-dependent up-regulation of cCRY1 and cCRY2 transcripts. *Neurosci. Lett.* 313:13–16.

73. Lin, C., M. Ahmad, and A. R. Cashmore. 1996. Arabidopsis cryptochrome 1 is a soluble protein mediating blue light-dependent regulation of plant growth and development. *Plant J.* 10:893–902.

74. Todo, T., H. Ryo, K. Yamamoto, H. Toh, T. Inui, H. Ayaki, T. Nomura, and M. Ikenaga. 1996. Similarity among the Drosophila (6–4)photolyase, a human photolyase homolog, and the DNA photolyase-blue-light photoreceptor family. *Science.* 272:109–112.

75. Todo, T., S. T. Kim, K. Hitomi, E. Otoshi, T. Inui, H. Morioka, H. Kobayashi, E. Ohtsuka, H. Toh, and M. Ikenaga. 1997. Flavin adenine dinucleotide as a chromophore of the Xenopus (6–4)photolyase. *Nucleic Acids Res.* 25:764–768.

76. Nakajima, S., M. Sugiyama, S. Iwai, K. Hitomi, E. Otoshi, S. T. Kim, C. Z. Jiang, T. Todo, A. B. Britt, and K. Yamamoto. 1998. Cloning and characterization of a gene (UVR3) required for photorepair of 6–4 photoproducts in Arabidopsis thaliana. *Nucleic Acids Res.* 26: 638–644.